Speckle reduction of retinal optical coherence tomography based on contourlet shrinkage

Jianbing Xu,[1] Haiyan Ou,[1,2] Edmund Y. Lam,[1] P. C. Chui,[1] and Kenneth K. Y. Wong[1]

[1]*Department of Electrical and Electronic Engineering, The University of Hong Kong, Pokfulam Road, Hong Kong*

[2]*Institue of Applied Physics, University of Electronic Science and Technology of China, Chengdu, China*

**Corresponding author: kywong@eee.hku.hk*

Received June 4, 2013; accepted July 8, 2013;
posted July 15, 2013 (Doc. ID 191738); published July 31, 2013

Speckle reduction of retinal optical coherence tomography (OCT) images helps the diagnosis of ocular diseases. In this Letter, we present a speckle reduction method based on shrinkage in the contourlet domain for retinal OCT images. The algorithm overcomes the disadvantages of the wavelet shrinkage method, which lacks directionality and anisotropy. The trade-off between speckle reduction and edge preservation is controlled by a single adjustable parameter, which determines the threshold in the contourlet domain. Results show substantial reduction of speckle noise and enhanced visualization of layer structures as demonstrated in the image of the central fovea region of the human retina. It is expected to be utilized in a wide range of biomedical imaging applications.

OCIS codes: (170.1610) Clinical applications; (170.4500) Optical coherence tomography; (110.6150) Speckle imaging; (100.2980) Image enhancement.

http://dx.doi.org/10.1364/OL.38.002900

Optical coherence tomography (OCT) [1], as an emerging noninvasive optical imaging modality allowing for high-resolution imaging of the retina microstructure and morphology, has been well demonstrated [2–5]. Further quantitative image analysis such as retinal layer segmentation [3,4] facilitates the quantification of retinal layers from the nerve fiber layer to the pigment epithelium layer. Retinal layer thickness derived from such image analysis methods may improve the clinical diagnosis during glaucoma progression and age-related macular degeneration [4,5]. However, retinal OCT images are severely degraded due to the presence of speckle noise [6], which causes difficulty in the precise identification of the layer boundaries. The accuracy of segmentation algorithms, which can be used to assess macular edema and nerve fiber atrophy, is reduced by speckle noise.

Wavelet shrinkage techniques have been employed successfully in speckle noise reduction for OCT images [7–11]. By transforming the OCT image into the wavelet domain, speckle noise is usually coded by small wavelet coefficients while signals are coded by large ones. By keeping large coefficients and suppressing small ones, speckle noise can be effectively attenuated. Whereas wavelet transform has been widely applied to despeckle OCT images, it only recognizes one-dimensional (1D) image singularities effectively and does not capture the geometrical smoothness of the image contours [12,13], which are of significant importance for retinal OCT images as a way for clinical measure of retinal disease progression. Wavelet representation is therefore not optimal and only shows limited performance in despeckling the retinal OCT images.

Recently, a new multiscale and multidirectional image representation method named contourlet transform has been proposed [14]. It is regarded as a "true" two-dimensional (2D) image representation as it can more effectively capture image edges and contours. The rationale is that it can represent the image contours and edges with a few number of large transformed coefficients, and noise is more spread out and coded by smaller ones. Moreover, the high degree of directionality and anisotropy offered by contourlet transform makes it superior to wavelet transform, which decomposes data into only three directions. The directional selectivity is improved by using dual-tree complex wavelet transform compared with discrete wavelet transform; it, however, is still limited to six distinct directions [10]. Therefore, we believe that it is more suited to use contourlet transform for retinal OCT image despeckling.

In this Letter, we present for the first time a speckle reduction technique based on contourlet transform for ophthalmic OCT images despeckling. Our results justify that the contourlet transform can be an effective tool in denoising ophthalmic OCT images.

There are different versions of contourlet transform. We use the nonredundant and orthogonal version, which has been described in detail elsewhere [14], for both the forward and inverse transformations. In brief, the forward contourlet transform consists of two major stages: the subband decomposition and the directional transform. It is first constructed by a Laplacian pyramid (LP) subband decomposition followed by directional filter banks (DFBs) applied on each subband. The LP decomposes the image into different octave frequency subbands, while the DFB decomposes each LP subband into many directions. The LP subbands and DFB provide scale and direction information of image signals, respectively. The contourlet transform allows for different and flexible number of directions at each scale.

The proposed contourlet shrinkage procedure closely emulates the despeckling method of wavelet shrinkage, which is denoising by thresholding the wavelet coefficients in the wavelet domain [7,10]. It is achieved in the contourlet domain and consists of four steps: forward contourlet transform, threshold estimation, threshold shrinkage, and inverse contourlet transform. A logarithmic transformation has to be performed prior to this procedure to convert the multiplicative speckle noise into additive noise. On a logarithmic scale, the observed

image Y is modeled as uncorrupted image S and additive speckle noise E:

$$Y = S + E. \tag{1}$$

Then a forward contourlet transform is performed on the noisy image Y. The transformed coefficient is a function of the scale i, the direction j, and the spatial coordinate x and y. The contourlet coefficients are represented as

$$Y_{i,j,x,y} = S_{i,j,x,y} + E_{i,j,x,y}, \tag{2}$$

where $Y_{i,j,x,y}$ are contourlet coefficients for the noisy image, $S_{i,j,x,y}$ are uncorrupted coefficients, and $E_{i,j,x,y}$ are the noise contributions. Following that, an estimated hard threshold $T_{i,j}$ is performed to each contourlet coefficient $Y_{i,j,x,y}$ such that

$$\hat{Y}_{i,j,x,y} = \begin{cases} Y_{i,j,x,y} & \text{if } |Y_{i,j,x,y}| \geq T_{i,j} \\ 0 & \text{otherwise,} \end{cases} \tag{3}$$

where $\hat{Y}_{i,j,x,y}$ denotes the denoised coefficients. Then, the inverse contourlet transform is performed on the new contourlet coefficients $\hat{Y}_{i,j,x,y}$ to reconstruct the denoised image.

The estimation of the threshold value is based upon the noise variance of the corrupted image. The contourlet coefficients in each subband are assumed to form a zero-mean generalized Gaussian distribution [15]. To obtain a threshold, we leverage the Monte Carlo method [16,17]: $T_{i,j} = K\sigma_1\sigma_2$, where σ_1 is the standard deviation of speckle noise in the image, and σ_2 is standard deviation of speckle noise in the contourlet domain at a specific scale i and direction j by Monte Carlo analysis. In order to account for the slight noise estimation deviation from the actual speckle noise distribution, an adjustable parameter K is introduced [17] to further reduce noise with a minimal effect on the edge sharpness. The value of K is usually obtained by trial and error, and it controls the degree of speckle reduction. The trade-off between speckle reduction and edge preservation, therefore, is achieved by tuning a single parameter.

The proposed method was applied to a spectral domain (SD) ophthalmic OCT image. The SD-OCT system (*Vivolight* LTD, China) uses a superluminescent diode of 840 nm and allows the capture of 30,000 A-scans/s, with an axial and lateral resolution of 8 and 15 μm, respectively. The sensitivity is 102 dB with 800 μW light incident on the sample. Figure 1(a) shows the original noisy image (512×256), which was centered on the fovea in order to image the macular region of human retina.

Here, we used three–scale decompositions of contourlet transform, where the image was decomposed into a low passband and 8, 16, and 16 directional bands, respectively. It should be noted that the number of directions doubles every other scale [14]. To remove Gibbs artifacts in the contourlet coefficients, cycle spinning [18] was also applied. A universal threshold is used for all scales and directions and the value of K is 0.6.

The unprocessed OCT image, shown in Fig. 1(a), has a grainy appearance because of the presence of speckle noise. As shown in Fig. 1(c), much of the speckle noise

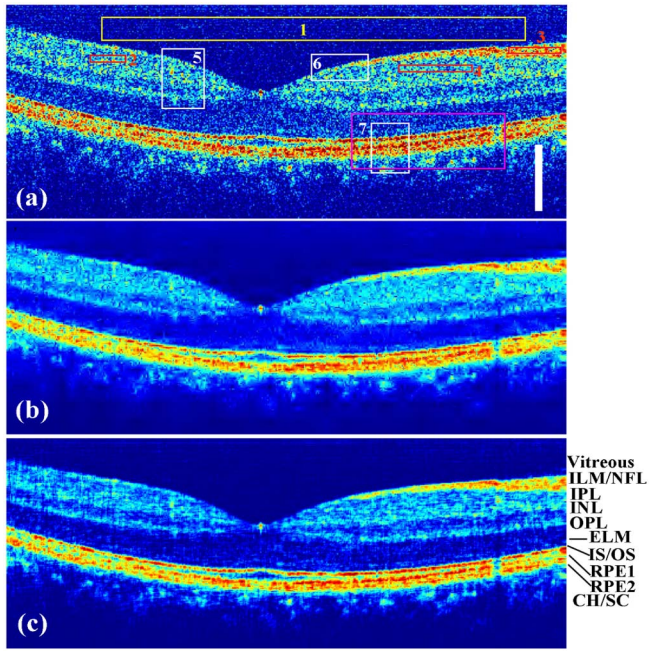

Fig. 1. Cross-sectional images of the central fovea region of the human retina. (a) Original noisy image, (b) image after wavelet-based speckle reduction, and (c) image after contourlet-based speckle reduction. For direct comparison, images are shown on the same color scale. ILM/NFL, inner limiting membrane/nerve fiber layer; IPL, inner plexiform layer; INL, inner nuclear layer; OPL, outer plexiform layer; ELM, external limiting membrane; IS/OS, junction between the inner and outer segment of the photoreceptors; RPE, retinal pigment epithelium; CH/SC junction between the choroid and sclera. The scale bar represents 200 μm.

in the original image has been suppressed by using contourlet shrinkage, improving the visualization of small morphological features. The reduction of the surrounding noise allows the features in the image to be more clearly delineated, such as the inner limiting membrane/nerve fiber layer and inner plexiform layer. The outer plexiform layer is also more discernible. For comparison, we also performed undecimated wavelet-based thresholding [12], as shown in Fig. 1(b). The threshold is chosen to be 3.1 times the noise variance, which is obtained from the robust median estimator of the highest subband of the transform [12,17]. The number 3.1 is chosen so that the edge preservation of the wavelet-based despeckled image is the same as that of the contourlet-based despeckled image.

In addition to the noise reduction, the despeckled image appears with enhanced visibility of retinal layers. To better appreciate how the contourlet shrinkage method improves the discernibility of the image contours and edges, Fig. 2 shows a zoom-in view of the pink region of interest (ROI) in Fig. 1(a). As indicated in Fig. 2(a), The inner and outer segment of the photoreceptors (IS/OS) and retinal pigment epithelium (RPE) did not show nicely continuous layers, and RPE1 and RPE2 cannot be easily resolved from each other owing to the presence of speckle noise. After contourlet shrinkage speckle reduction, the layered structure in the image can be more clearly delineated. The IS/OS contours are nicely depicted and the RPE1 and RPE2 can be easily

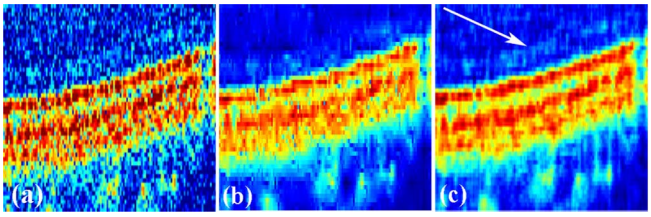

Fig. 2. (a) Enlarged view of the pink ROI in the original noisy image, (b) enlarged view of the pink ROI processed by wavelet shrinkage, and (c) enlarged view of the pink ROI processed by contourlet shrinkage.

discerned. For the wavelet shrinkage method, as shown in Fig. 2(b), the IS/OS edges are distorted and the RPE1-RPE2 cannot be resolved easily. Moreover, the external limiting membrane (ELM), where the white arrow resides, is too weak and can hardly be observed in the original noisy image, whereas it, though not distinct, becomes observable after despeckling using contourlet shrinkage. For the despeckled image by wavelet shrinkage, on the contrary, the weak ELM signals are attenuated. The reason for this performance difference is that wavelet transform is only optimal in representing 1D singularities, but not optimal for 2D image contours or layers as it lacks directionality and anisotropy. On the other hand, contourlet transform is optimal in representing 2D image contours or layers. As a result, the contourlet transform would generate relatively larger transformed coefficients for such continuous features as ELM, while the wavelet coefficients for the weak ELM signals are small and are easily attenuated along with speckle noise. Retinal layers and edges play an important role in accurately measuring cellular disruption for retinal pathology. The proposed contourlet shrinkage method, therefore, is a highly promising preprocessing approach which yields enhanced retinal OCT image quality for further quantitative analysis, such as retina layer segmentation. Less ambiguity of the retinal layer structures after despeckling will enable more accurate segmentation results.

Image quality metrics were used to assess the quantitative performance of the despeckling technique by measuring the SNR, contrast-to-noise ratio (CNR), the equivalent number of looks (ENL), and edge preservation over ROIs. These metrics have been described in detail elsewhere [7,8]. Briefly, CNR measures the contrast between image features and noise. ENL measures the smoothness of areas that should have a homogeneous appearance but are corrupted by speckle noise. Edge preservation parameter β measures how much the edge sharpness has degraded as a result of the denoising process. The larger the parameter β, the more edges are preserved.

Seven ROIs were manually selected and overlaid in the original image, as shown in Fig. 1(a). The ROIs, which include three homogeneous ones (three red boxes labeled 2, 3, and 4), three inhomogeneous ones (three white boxes labeled 5, 6, and 7), and a background region (one yellow box labeled 1, for the retinal image it is the vitreous-humor area), were chosen to cover different retinal layers and edges, and were used for different measurements. The metrics were calculated as the average over the ROIs. The CNR values were averaged over six ROIs (2–7). The ENL values were averaged over the three homogeneous ROIs (2–4). The first ROI was used to calculate the background noise level. Table 1 lists the respective results of the quality metrics when $K = 0.4$, 0.6, and 1. As expected, in all cases, the SNR, CNR, and ENL all show improvement compared with the original image. The application of the contourlet shrinkage ($K = 0.6$) results in an improvement of ENL by a factor of 4 times. CNR and SNR improvement are also observed. The CNR improves by 1.52 dB and the SNR improves by 16.53 dB. Most importantly, all of these are achieved with a degradation of edge preservation parameter β by only 6.8% (0.932). The results demonstrate the effectiveness of the proposed approach for speckle noise reduction with signals well preserved simultaneously. Comparing contourlet-based and wavelet-based methods, for a similar edge preservation value ($K = 0.6$), our contourlet-based method further improves the SNR, CNR, and ENL by 1.53 dB, 0.22 dB, and 2.39 times, respectively.

Table 1. Image Quality Metrics

	SNR (dB)	CNR (dB)	ENL	Beta
Original	29.39	1.30	25.05	N/A
Contourlet, $K = 0.4$	43.50	2.43	58.95	0.959
Contourlet, $K = 0.6$	45.92	2.82	108.67	0.932
Contourlet, $K = 1$	50.68	3.27	129.55	0.895
Wavelet	44.39	2.60	45.39	0.932

To further illustrate how the parameter K controls the degree of speckle reduction, Fig. 3 shows the CNR and edge preservation parameter β for various choices of K, illustrating the trade-off between edge sharpness preservation and speckle reduction, by simply tuning the parameter K.

The rationale for the superior performance of contourlet shrinkage in speckle reduction over wavelet shrinkage lies in the directionality and anisotropy property of the contourlet transform, which allows for different and flexible number of directions at each scale. Therefore, one can take advantage of the direction selectivity of the contourlets and adjust the threshold in any direction to optimize the image quality between speckle reduction and edge preservation. For example, when signals are mainly concentrated along certain directions, one

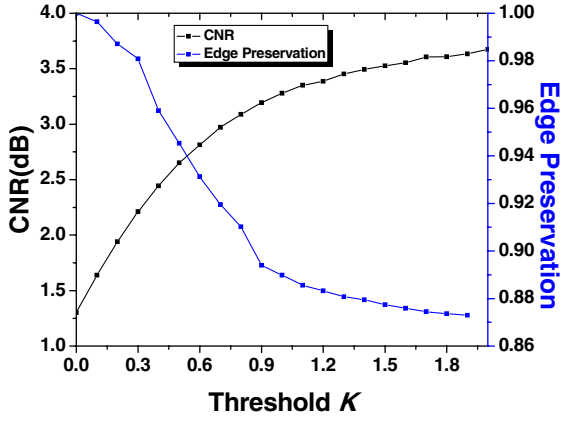

Fig. 3. CNR and edge preservation parameter β as a function of different threshold K.

can choose to set a small threshold for those directions to preserve more signals while a large threshold can be used for other directions to suppress more noise. Furthermore, the algorithm was computationally efficient. The total time for the despeckling process was 11.4 s by implementing on an Intel Core i5 computer using MATLAB. Further acceleration may require implementation in C + + and/or GPU parallel processing.

In conclusion, we presented, to our knowledge, for the first time how speckle reduction based on contourlet shrinkage can potentially benefit retinal OCT image quality by enhancing visibility of retinal morphological structures. It is demonstrated that by tuning a single parameter, trade-off between speckle reduction and edge preservation can be achieved. Furthermore, the proposed contourlet shrinkage method shows optimal preservation of image edges and contours, which is useful for quantitative image analysis, such as image layer segmentation for clinical ocular diseases diagnosis. Hence, it is expected to be utilized in a wide range of biomedical imaging applications.

The authors acknowledge the help of Mr. Rui Zhu from Shenzhen *Vivolight* Medical Device, LTD, China. This research was partially supported by the Research Grants Council of the Hong Kong Special Administrative Region, China (Project No. HKU 7172/12E), and the National Natural Science Foundation of China under grants 61107018.

References

1. D. Huang, E. A. Swanson, C. P. Lin, J. S. Schuman, W. G. Stinson, W. Chang, M. R. Hee, T. Flotte, K. Gregory, C. A. Puliafito, and J. G. Fujimoto, Science **254**, 1178 (1991).
2. J. G. Fujimoto, W. Drexler, J. S. Schuman, and C. K. Hitzenberger, Opt. Express **17**, 3978 (2009).
3. A. Mishra, A. Wong, K. Bizheva, and D. A. Clausi, Opt. Express **17**, 23719 (2009).
4. Q. Yang, C. A. Reisman, Z. Wang, Y. Fukuma, M. Hangai, N. Yoshimura, A. Tomidokoro, M. Araie, A. S. Raza, and D. C. Hood, Opt. Express **18**, 21293 (2010).
5. S. Taliantzis, D. Papaconstantinou, C. Koutsandrea, M. Moschos, M. Apostolopoulos, and G. Georgopoulos, Clin. Ophthalmol. **3**, 373 (2009).
6. J. M. Schmitt, S. Xiang, and K. M. Yung, J. Biomed. Opt. **4**, 95 (1999).
7. D. C. Adler, T. H. Ko, and J. G. Fujimoto, Opt. Lett. **29**, 2878 (2004).
8. P. Puvanathasan and K. Bizheva, Opt. Express **15**, 15747 (2007).
9. A. Pižurica, L. Jovanov, B. Huysmans, V. Zlokolica, P. de Keyser, F. Dhaenens, and W. Philips, Curr. Med. Imaging Rev. **4**, 270 (2008).
10. S. Chitchian, M. A. Fiddy, and N. M. Fried, J. Biomed. Opt. **14**, 014031 (2009).
11. M. A. Mayer, A. Borsdorf, M. Wagner, J. Hornegger, C. Y. Mardin, and R. P. Tornow, Biomed. Opt. Express **3**, 572 (2012).
12. D. L. Donoho and I. M. Johnstone, J. Am. Stat. Assoc. **90**, 1200 (1995).
13. S. Mallat, *A Wavelet Tour of Signal Processing* (Academic, 1998).
14. M. N. Do and M. Vetterli, IEEE Trans. Image Process. **14**, 2091 (2005).
15. D. D. Y. Po and M. N. Do, IEEE Trans. Image Process. **15**, 1610 (2006).
16. J.-L. Starck, E. J. Candès, and D. L. Donoho, IEEE Trans. Image Process. **11**, 670 (2002).
17. Z. Jian, Z. Yu, L. Yu, B. Rao, Z. Chen, and B. J. Tromberg, Opt. Lett. **34**, 1516 (2009).
18. R. R. Coifman and D. L. Donoho, *Translation Invariant Denoising* (Springer, 1995).